Proceedings of the 17th World Congress
The International Federation of Automatic Control
Seoul, Korea, July 6-11, 2008

Interconnection and Damping Assignment Passivity–Based Control of the Pendubot [1]

Jesús Sandoval *, **Romeo Ortega** ** and **Rafael Kelly** ***

* *Departamento Metal-Mecánica, Instituto Tecnológico de La Paz, Blvd. Forjadores de B.C.S. No. 4720, La Paz, B.C.S., 23080, MEXICO*
e–mail: jsandoval@marinos.itlp.edu.mx
** *Laboratoire des Signaux et Systèmes, CNRS-SUPELEC, Gif-sur-Yvette 91192, FRANCE*
e–mail: Romeo.Ortega@lss.supelec.fr

*** *División de Física Aplicada, CICESE, Carretera Tijuana–Ensenada km. 107, Ensenada, B. C., 22800, MEXICO*
e–mail: rkelly@cicese.mx
Fax: + 52 (646) 175 05 54

Abstract: In this paper, we apply the interconnection and damping assignment passivity–based control design technique to the underactuated mechanical system called *pendubot*. The proposed control system drives a class of pendubot systems to the upward configuration, starting from a neighborhood of this configuration. Simulation results show the performance of the proposed control system.

Keywords: Underactuated mechanical systems, Hamiltonian systems, stabilization, pendubot.

1. INTRODUCTION

The Interconnection and Damping Assignment (IDA) method —a formulation of Passivity–Based Control (PBC) —introduced in recent years by Ortega *et al.* [2002] is a control design methodology that assigns a suitable dynamics in closed–loop, being the Hamiltonian formulation the natural framework of this methodology. The main challenge of the IDA–PBC method consists in solving a set of equations, so–called *matching equations*, whose solutions determine the IDA–PBC control law. In the case of the underactuated mechanical systems —those that have more degree-of-freedom than inputs of control— the matching equations represent a set of partial differential equations (PDE's), whose solution is, in general, a difficult task.

Recently, in Acosta *et al.* [2005], the authors have shown a strategy that allows to convert the PDE's into a set of algebraic equations, incorporating additional free terms to ease the solution of these latter equations. In this paper, we apply this strategy to the control of the underactuated mechanical system *pendubot* –name coined by Spong and Block [1995]. Our main contribution is to present the design of an IDA–PBC control system that achieves to control a class of pendubot systems in completely upward position, starting from a neighborhood of this configuration.

The rest of the paper is organized as follows: In Section 2, we present a brief review of the IDA–PBC method applied to the stabilization of a class of underactuated mechanical systems. The model, the control objective and the design of the IDA–PBC control system proposal are described in Section 3. Simulations results of a pendubot are given in Section 4. Finally, we offer some concluding remarks in Section 5.

2. THE IDA–PBC METHOD

In this section, we present a brief review of the IDA–PBC method applied to the control of a class of underactuated mechanical systems. The interested reader is referred to Ortega *et al.* [2002] for further details. The procedure takes–off from a Hamiltonian description of the system with the total energy function given by the sum of the kinetic plus potential energies [2]

$$H(\boldsymbol{q},\boldsymbol{p}) = \frac{1}{2}\boldsymbol{p}^{\mathrm{T}}M^{-1}(\boldsymbol{q})\boldsymbol{p} + V(\boldsymbol{q}) \tag{1}$$

where $\boldsymbol{q} \in \mathbb{R}^n$ and $\boldsymbol{p} \in \mathbb{R}^n$ are the vectors of generalized position and momenta, respectively, $M = M^T > 0$ is the inertia matrix and V is the potential energy. If we assume that the system has no natural damping, the equations of motion can be written as

$$\frac{d}{dt}\begin{bmatrix}\boldsymbol{q}\\ \boldsymbol{p}\end{bmatrix} = \begin{bmatrix}\mathbf{0} & I_n\\ -I_n & \mathbf{0}\end{bmatrix}\begin{bmatrix}\nabla_{\boldsymbol{q}} H\\ \nabla_{\boldsymbol{p}} H\end{bmatrix} + \begin{bmatrix}\mathbf{0}\\ G(\boldsymbol{q})\end{bmatrix}\boldsymbol{u} \tag{2}$$

[1] Work partially supported by CONACyT grant 45826 and by DGEST grant PAZ-CBAS-2007-02.

[2] To simplify notation, from now on for all expressions, which are functions of $\boldsymbol{q}$ and $\boldsymbol{p}$, we will write explicitly their dependence only the first time they are defined.

978-1-1234-7890-2/08/$20.00 © 2008 IFAC

10.3182/20080706-5-KR-1001.3640

being $\boldsymbol{u} \in \mathbb{R}^m$ the vector of control inputs with rank $G = m < n$ and $\nabla_{(\cdot)} = \frac{\partial}{\partial(\cdot)^T}$. The IDA–PBC method assigns a particular desired structure in closed–loop, preserving the Hamiltonian structure in (2), with a desired energy function given by

$$H_d(\boldsymbol{q},\boldsymbol{p}) = \frac{1}{2}\boldsymbol{p}^{\mathrm{T}} M_d^{-1}(\boldsymbol{q})\boldsymbol{p} + V_d(\boldsymbol{q}) \tag{3}$$

where $M_d = M_d^T > 0$ and V_d are the desired inertia matrix and the potential energy function, respectively. The desired closed–loop system is

$$\frac{d}{dt}\begin{bmatrix}\boldsymbol{q}\\ \boldsymbol{p}\end{bmatrix} = \begin{bmatrix}\mathbf{0} & M^{-1}M_d \\ -M_dM^{-1} & J_2(\boldsymbol{q},\boldsymbol{p}) - GK_vG^T\end{bmatrix}\begin{bmatrix}\nabla_{\boldsymbol{q}} H_d\\ \nabla_{\boldsymbol{p}} H_d\end{bmatrix} \tag{4}$$

where $J_2 = -J_2^T$ and $K_v = K_v^T > \mathbf{0}$ are *free* matrices. Now, for this class of Hamiltonian systems, the main challenge of the IDA–PBC method consists in solving the following set of PDE's, called *matching equations*,

$$\mathcal{G}\left\{\nabla_{\boldsymbol{q}}\left(\boldsymbol{p}^T M^{-1}\boldsymbol{p}\right) - M_dM^{-1}\nabla_{\boldsymbol{q}}\left(\boldsymbol{p}^T M_d^{-1}\boldsymbol{p}\right) + 2J_2M_d^{-1}\boldsymbol{p}\right\} = \mathbf{0} \tag{5}$$

$$\mathcal{G}\left\{\nabla_{\boldsymbol{q}}V - M_dM^{-1}\nabla_{\boldsymbol{q}}V_d\right\} = \mathbf{0} \tag{6}$$

where $\mathcal{G} = [G[G^TG]^{-1}G^T - I_n]$, whose solutions M_d and V_d define the control law given by

$$\boldsymbol{u} = [G^TG]^{-1}G^T\left[\nabla_{\boldsymbol{q}}H - M_dM^{-1}\nabla_{\boldsymbol{q}}H_d + J_2M_d^{-1}\boldsymbol{p}\right] - K_vG^TM_d^{-1}\boldsymbol{p} \tag{7}$$

Further, if M_d is positive definite in a neighborhood of $\boldsymbol{q}^*$, and

$$\boldsymbol{q}^* = \arg\min\{V_d\}$$

then $[\boldsymbol{q}^T \;\; \boldsymbol{p}^T]^T = [\boldsymbol{q}^{*T} \;\; \mathbf{0}^T]^T$ is a stable equilibrium of (4) with a Lyapunov function H_d. This equilibrium is asymptotically stable if it is locally detectable from the output $G^T\nabla_{\boldsymbol{p}}H_d$.

3. THE PENDUBOT

The *Pendubot* is an underactuated mechanical system consisting of two links that can move freely on a vertical plane through a pair of revolute joints. The first joint is endowed with an actuator that apply a torque on it, while the absence of actuaction in the second joint determine the underactuated nature of mechanism. A schematic picture of the pendubot is shown in Fig. 1, where q_1 and q_2 are the joint positions. The parameters of the two links are given by the lenght of the link l_i, the lenght at the center of mass l_{c_i}, the inertia momentum I_i and the mass m_i, with $i = 1, 2$. The gravity acceleration is given by g, while u is the torque applied on the first joint.

3.1 Model and control objective

The Hamiltonian model of the pendubot shown in Fig. 1, can be described by (2) with the matrices

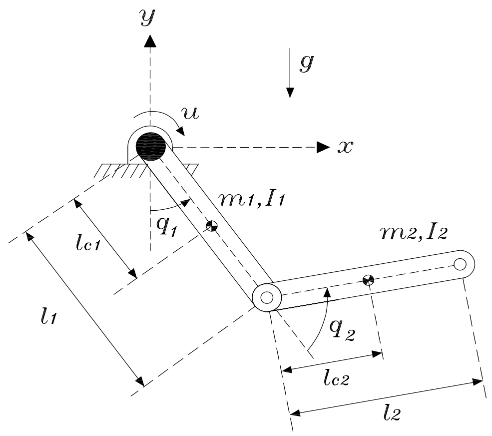

Fig. 1. Pendubot.

$$M(q_2) = \begin{bmatrix} c_1 + c_2 + 2c_3\cos(q_2) & c_2 + c_3\cos(q_2) \\ c_2 + c_3\cos(q_2) & c_2\end{bmatrix}$$
$$G = \begin{bmatrix}1\\0\end{bmatrix} \tag{8}$$

and the potential energy function

$$V(q_1,q_2) = -c_4 g\cos(q_1) - c_5 g\cos(q_1+q_2)$$

where the constants c_i, $i = 1, 2, \cdots, 5$, are defined as

$$\begin{array}{ll} c_1 = m_1l_{c_1}^2 + m_2l_1^2 + I_1, & c_2 = m_2l_{c_2}^2 + I_2,\; c_3 = m_2l_1l_{c_2} \\ c_4 = m_1l_{c_1} + m_2l_1, & c_5 = m_2l_{c_2}. \end{array} \tag{9}$$

For convenience of notation, the elements of the matrix M given in (8) are named as follows

$$M \triangleq \begin{bmatrix}a_1 & a_2\\ a_2 & a_3\end{bmatrix} \tag{10}$$

In words, the control objective is to drive the pendubot in the upward configuration, starting from a neighborhood of this configuration, where the desired position of the second link around the upright position always is parallel to the y axis shown in Fig. 1.

Formally, the control objective can be established as

$$\lim_{t\to\infty}\begin{bmatrix}q_1(t)\\ q_2(t)\end{bmatrix} = \begin{bmatrix}q_{d_1}\\ \pi - q_{d_1}\end{bmatrix} \tag{11}$$

where q_{d_1} is the desired position of the first joint, such that $\pi + \varepsilon > q_{d_1} > \pi - \varepsilon$, being $\varepsilon < \frac{\pi}{2}$ a positive constant determined by the parameters of the pendubot.

3.2 IDA–PBC control design

Inspired by the work of Acosta *et al.* [2005], in this subsection we present in detail the design of the IDA–PBC control law of the pendubot to satisfy the control objective (11).

First, we apply the results shown in section 2, where

$$\boldsymbol{q} = [q_1 \;\; q_2]^T,\; \boldsymbol{p} = [p_1 \;\; p_2]^T,\; \mathcal{G} = \begin{bmatrix}0 & 0\\ 0 & 1\end{bmatrix}$$

and from now on, we will denote $G^{\perp} = [0 \;\; 1]$ as the second row of $\mathcal{G}$. Notice that it is such that $G^{\perp}G = 0$. Next, the assignment of $M_d = M_d(q_2)$ will ease the solution of the algebraic equations, such as we will see more latter. A key step in our design is the particular assignment of the matrix

$$J_2 = \begin{bmatrix} 0 & \tilde{\boldsymbol{p}}^T\boldsymbol{\alpha}(q_2) \\ -\tilde{\boldsymbol{p}}^T\boldsymbol{\alpha}(q_2) & 0 \end{bmatrix} = \tilde{\boldsymbol{p}}^T\boldsymbol{\alpha}W \qquad (12)$$

being $\tilde{\boldsymbol{p}} = M_d^{-1}\boldsymbol{p}$, $\boldsymbol{\alpha} = [\alpha_1(q_2) \quad \alpha_2(q_2)]^T$ *free* and $W \in so(2)$. With M_d and J_2 matrices, and utilizing the identity

$$\frac{dM^{-1}}{dq_i} = -M^{-1}\frac{dM}{dq_i}M^{-1}$$

equation (5) yields

$$-\boldsymbol{p}^T M^{-1}\frac{dM}{dq_2}M^{-1}\boldsymbol{p} + G^{\perp}M_dM^{-1}e_2\boldsymbol{p}^TM_d^{-1}\frac{dM_d}{dq_2}M_d^{-1}\boldsymbol{p} + 2\boldsymbol{p}^TM_d^{-1}\boldsymbol{\alpha}G^{\perp}WM_d^{-1}\boldsymbol{p} = 0 \quad (13)$$

where e_2 is the base vector. Now, (13) can be expressed as

$$\boldsymbol{p}^T\left[-M^{-1}\frac{dM}{dq_2}M^{-1} + [G^{\perp}M_dM^{-1}e_2]M_d^{-1}\frac{dM_d}{dq_2}M_d^{-1} - M_d^{-1}\begin{bmatrix} 2\alpha_1 & \alpha_2 \\ \alpha_2 & 0 \end{bmatrix}M_d^{-1}\right]\boldsymbol{p} = 0 \qquad (14)$$

such that we have assigned uniquely the symmetric part of the matrix $2\boldsymbol{\alpha}G^{\perp}W$, given by $\mathcal{A} = \boldsymbol{\alpha}G^{\perp}W + [\boldsymbol{\alpha}G^{\perp}W]^T$, this is,

$$2\boldsymbol{\alpha}G^{\perp}W = -2\begin{bmatrix} \alpha_1 & 0 \\ \alpha_2 & 0 \end{bmatrix} = \underbrace{-\begin{bmatrix} 2\alpha_1 & \alpha_2 \\ \alpha_2 & 0 \end{bmatrix}}_{\mathcal{A}} - \begin{bmatrix} 0 & -\alpha_2 \\ \alpha_2 & 0 \end{bmatrix}$$

It's easy to verify that $2G^{\perp}J_2M_d^{-1}\boldsymbol{p} = \boldsymbol{p}^TM_d^{-1}\mathcal{A}M_d^{-1}\boldsymbol{p}$, with J_2 given by (12). It is worth to remark that the assignment of matrix $\mathcal{A}$ is crucial in our design. A detailed analysis of the incorporation of this novel matrix in the solution of (5) is shown in Acosta *et al.* [2005]. Next, from (14) we have

$$-M^{-1}\frac{dM}{dq_2}M^{-1} + [G^{\perp}M_dM^{-1}e_2]M_d^{-1}\frac{dM_d}{dq_2}M_d^{-1} - M_d^{-1}\begin{bmatrix} 2\alpha_1 & \alpha_2 \\ \alpha_2 & 0 \end{bmatrix}M_d^{-1} = 0$$

which pre-multiplying and post-multiplying by M_d and defining $\Lambda = \begin{bmatrix} \lambda_1 & \lambda_2 \\ \lambda_3 & \lambda_4 \end{bmatrix} \triangleq M_dM^{-1}$, yields

$$c_3\sin(q_2)\Lambda\begin{bmatrix} 2 & 1 \\ 1 & 0 \end{bmatrix}\Lambda^T + \lambda_4\frac{dM_d}{dq_2} - \begin{bmatrix} 2\alpha_1 & \alpha_2 \\ \alpha_2 & 0 \end{bmatrix} = 0 \quad (15)$$

Before going on, it's convenient to tell that until now, the strategy of design that we have followed seeks to ease the solution of M_d in (5). In our case the set of PDE's shown in (5) has been transformed into the set of algebraic equations in (15), which present no obstacle in the solution of M_d, because α_1 and α_2 are free.

Now, we continue our design considering from the definition of the matrix Λ, that

$$M_d = \Lambda M \triangleq \begin{bmatrix} d_1 & d_2 \\ d_3 & d_4 \end{bmatrix}$$

where

$$\begin{aligned} d_1 &= \lambda_1[c_1 + c_2 + 2c_3\cos(q_2)] + \lambda_2[c_2 + c_3\cos(q_2)] \\ d_2 &= \lambda_1[c_2 + c_3\cos(q_2)] + \lambda_2c_2 \\ d_3 &= \lambda_3[c_1 + c_2 + 2c_3\cos(q_2)] + \lambda_4[c_2 + c_3\cos(q_2)] \\ d_4 &= \lambda_3[c_2 + c_3\cos(q_2)] + \lambda_4c_2 \end{aligned} \quad (16)$$

Taking into account (16) in (15), results in the set of algebraic equations given by (17), (18) and (19), all showed in the next page. While that from (6), results in the next PDE

$$\lambda_3\nabla_{q_1}V_d + \lambda_4\nabla_{q_2}V_d = c_5g\sin(q_1 + q_2). \qquad (20)$$

Algebraic equations and PDE solutions A suitable assignment of λ_3 and λ_4 constants, allows to solve (19) with $\lambda_3 = k_3$ and $\lambda_4 = -2k_3$, being k_3 an arbitrary constant. Moreover, incorporating these results in (20) yields, later to solve the PDE (20),

$$V_d = \frac{c_5g}{k_3}\cos(q_1 + q_2) + \Phi(q_2 + 2q_1) \qquad (21)$$

where $\Phi(\cdot) \in C^1$ is free. The neccesity of $\boldsymbol{q}^* = \arg\min\{V_d\}$ require that V_d be positive definite in a neighborhood of $\boldsymbol{q}^*$. Towards this end, it can be verified that

$$V_d = \frac{c_5g}{k_3}[\cos(q_1+q_2)+1] + \frac{k_p}{2}[q_2+2q_1-(\pi+q_{d_1})]^2 \quad (22)$$

achieves the previous requirement, with k_p and k_3 positive constants. To prove the positivity of V_d, notice that the gradient of V_d is

$$\nabla_{\boldsymbol{q}}V_d = \begin{bmatrix} -\frac{c_5g}{k_3}\sin(q_1+q_2) + 2k_p[q_2+2q_1-(\pi+q_{d_1})] \\ -\frac{c_5g}{k_3}\sin(q_1+q_2) + k_p[q_2+2q_1-(\pi+q_{d_1})] \end{bmatrix}$$

whose solutions are $q_1 = (1-n)\pi + q_{d_1}$ and $q_2 = (2n-1)\pi - q_{d_1}$, with $n \in \mathbb{N}$. It's easy to verify that the Hessian of V_d is

$$\nabla^2_{\boldsymbol{q}}V_d = \begin{bmatrix} -\frac{c_5g}{k_3}\cos(q_1+q_2) + 4k_p & -\frac{c_5g}{k_3}\cos(q_1+q_2) + 2k_p \\ -\frac{c_5g}{k_3}\cos(q_1+q_2) + 2k_p & -\frac{c_5g}{k_3}\cos(q_1+q_2) + k_p \end{bmatrix}$$

which being evaluated at $(q_1 = q_{d_1}, q_2 = \pi - q_{d_1})$, results in

$$\nabla^2_{\boldsymbol{q}}V_d = \begin{bmatrix} \frac{c_5g}{k_3} + 4k_p & \frac{c_5g}{k_3} + 2k_p \\ \frac{c_5g}{k_3} + 2k_p & \frac{c_5g}{k_3} + k_p \end{bmatrix}$$

being positive definite with k_p and k_3 positives.

Positivity and symmetry of M_d Next, we proceed with the assignment of the elements of M_d that satisfy the requirement of positivity and symmetry of this matrix. Taking this into account, notice that from last two lines of (16), d_3 and d_4 are determined by λ_3 and λ_4 as

$$\begin{aligned} d_3 &= k_3[c_1 - c_2] \\ d_4 &= k_3[-c_2 + c_3\cos(q_2)] \end{aligned}$$

where a requirement for positivity of M_d is $d_4 > 0$, which is achieved for all

$$2c_3\sin(q_2)[\lambda_1^2+\lambda_1\lambda_2]+\lambda_4\frac{d}{dq_2}(\lambda_1[c_1+c_2+2c_3\cos(q_2)]+\lambda_2[c_2+c_3\cos(q_2)])-2\alpha_1=0 \tag{17}$$

$$c_3\sin(q_2)[2\lambda_1\lambda_3+\lambda_1\lambda_4+\lambda_2\lambda_3]+\lambda_4\frac{d}{dq_2}(\lambda_1[c_2+c_3\cos(q_2)]+\lambda_2c_2)-\alpha_2=0 \tag{18}$$

$$2c_3\sin(q_2)[\lambda_3^2+\lambda_3\lambda_4]+\lambda_4\frac{d}{dq_2}(\lambda_3[c_2+c_3\cos(q_2)]+\lambda_4c_2)=0 \tag{19}$$

$$q_2\in(-\varepsilon,\varepsilon) \tag{23}$$

being $\varepsilon = \arccos\left(\frac{c_2}{c_3}\right)$ with $c_3 > c_2$, implying this later that $\varepsilon < \frac{\pi}{2}$. It's worth remarking that the inequality

$$c_3 > c_2 \tag{24}$$

determine the class of pendubot systems to which applies the proposed IDA–PBC control system, because c_3 and c_2 are physical parameters of the pendubot. Moreover, the ε value bounds the initial position of the second link, such that the rest initial configuration of the pendubot must be above the horizontal. The latter can be verified from Fig. 1, because for all initial configuration —with zero velocity— below the x horizontal axis, the second link always drives downwards due to gravity force, independently of any movement of the first link. As consequence, in this case the stabilization of the pendubot is not possible, because q_2 doesn't meet anymore (23). Current research is in process to determine an explicity estimate of the domain of attraction with a well–defined set of initial conditions ensuring attractivity of the desired equilibrium.

On the other hand, from the first two lines of (16), the assignment of λ_1 and λ_2 is subject to the requirement that impose the positivity and symmetry of M_d on the elements d_1 and d_2. Taking into account this requirement, and having defined previously λ_3 and λ_4, we can rewrite $M_d = \Lambda M$ as

$$M_d = k_3\begin{bmatrix}\rho & \lambda_1^o a_2+\lambda_2^o a_3\\ a_1-2a_2 & a_2-2a_3\end{bmatrix}$$

where the elements λ_1 and λ_2 have been expressed conveniently as the product of k_3 by λ_1^o and λ_2^o, respectively, and ρ is given by

$$\rho = \lambda_1^o a_1+\lambda_2^o a_2. \tag{25}$$

Notice that the symmetry of M_d is determined by

$$\lambda_2^o = \frac{a_1-2a_2}{a_3}-\frac{a_2}{a_3}\lambda_1^o \tag{26}$$

while to ensure the positivity of M_d, we need that

$$\rho > \frac{[a_1-2a_2]^2}{a_2-2a_3} = \frac{[c_1-c_2]^2}{-c_2+c_3\cos(q_2)}$$

be positive, which is satisfied with

$$\rho > \frac{[c_1-c_2]^2}{-c_2+c_3\cos(\varepsilon-\mu)} \tag{27}$$

being $\mu << 1$. Afterwards, substituting (26) in (25), yields

$$\lambda_1^o = \frac{a_3\rho-a_2[a_1-2a_2]}{\Delta}.$$

Finally, with these results, the matrix M_d becomes

$$M_d = k_3\begin{bmatrix}\rho & c_1-c_2\\ c_1-c_2 & -c_2+c_3\,\cos(q_2)\end{bmatrix} \tag{28}$$

On the other hand, substituting the λ_i elements, in (17) and (18), we determine α_1 and α_2, as

$$\alpha_1 = c_3\sin(q_2)[\lambda_1^2+\lambda_1\lambda_2]$$

$$\alpha_2 = \frac{-k_3^2c_3\sin(q_2)[c_2\rho+c_2^2-2c_3\cos(q_2)[c_1-c_2]]}{c_1c_2-c_3^2\cos^2(q_2)} + \frac{c_3\cos(q_2)\rho-c_1^2}{c_1c_2-c_3^2\cos^2(q_2)}$$

Finally, the control law (7) yields

$$u = \nabla_1V-\left[\lambda_1\nabla_1V_d+\lambda_2\left[\frac{1}{2}\nabla_2(\boldsymbol{p}^TM_d^{-1}\boldsymbol{p})+\nabla_2V_d\right]\right] + \boldsymbol{p}^TM_d^{-1}\boldsymbol{\alpha}\left[\frac{-d_3p_1+d_1p_2}{\Delta_d}\right]-k_v\left[\frac{d_4p_1-d_2p_2}{\Delta_d}\right] \tag{29}$$

where $\Delta_d = d_1d_4-d_2d_3 > 0$, is the determinant of M_d, $k_v > 0$ is an arbitrary constant and the rest of terms are given by

$$\nabla_1V = c_4g\sin(q_1)+c_5g\sin(q_1+q_2)$$

$$\nabla_1V_d = -\frac{c_5g}{k_3}\sin(q_1+q_2)+2k_p[q_2+2q_1-(\pi+q_{d_1})]$$

$$\nabla_2(\boldsymbol{p}^TM_d^{-1}\boldsymbol{p}) = -\frac{k_3c_3\sin(q_2)p_1^2}{\Delta_d} + \frac{c_3\sin(q_2)\rho[d_4p_1^2-(d_2+d_3)p_1p_2+d_1p_2^2]}{k_3^2[(c_1-c_2)^2+c_2\rho-c_3\cos(q_2)\rho]^2}$$

$$\nabla_2V_d = -\frac{c_5g}{k_3}\sin(q_1+q_2)+k_p[q_2+2q_1-(\pi+q_{d_1})]$$

$$\boldsymbol{p}^TM_d^{-1}\boldsymbol{\alpha} = \frac{p_1[d_4\alpha_1-d_2\alpha_2]+p_2[-d_3\alpha_1+d_1\alpha_2]}{\Delta_d}$$

4. SIMULATIONS

In this section, we present simulation results obtained on a pendubot by using the parameters given in Wang-Sheng and Juang-Shan [2006], which belongs to the class of pendubot systems satisfying (24). The values of the model of the pendubot and the parameters of control system are indicated in the table 1.

Table 1. Parameters

Link 1	*Link 2*	*Gains*
$l_1 = 2$	$l_2 = 1$	$\rho = 500$
$m_1 = 2$	$m_2 = 1$	$k_3 = 0.0033$
$l_{c_1} = 1$	$l_{c_2} = 0.5$	$k_p = 30$
$I_1 = 0.667$	$I_2 = 0.083$	$k_v = 20$

In accordance with the parameters in the table 1, we obtain from (9) that $c_3 = 1$ and $c_2 = 0.333$, satisfying (24), while the ε value results

$$\varepsilon = \arccos\left(\frac{c_2}{c_3}\right) = 1.23\,[\text{rad}] < \frac{\pi}{2}.$$

We carried out a pair of simulations to verify the performance of the control system, considering in both simulations the gains given in table 1. The desired position in the first simulation was $q_{d_1} = \pi$ [rad], because we wish to put both links completely in an upright position. The initial configuration —starting above the horizontal with zero velocity— was $[q_1(0) \;\; q_2(0) \;\; p_1(0) \;\; p_2(0)]^T = [(\pi - 1.1) \;\; 1.1 \;\; 0 \;\; 0]^T$, which is reasonably far from the desired configuration. Notice that we have chosen $q_2(0) = 1.1\,[\text{rad}] = \varepsilon - \mu$, with $\mu = 0.13$. Therefore, to ensure the positivity of M_d, in accordance with (27), we have that $\rho > 332.7$. The pictures in Fig. 2 show the temporal evolution of joint positions and the control input. A simple observation shows as joint positions q_1 and q_2 converge toward the desired values $[q_1 \;\; q_2 \;\; p_1 \;\; p_2]^T = [\pi \;\; 0 \;\; 0 \;\; 0]^T$.

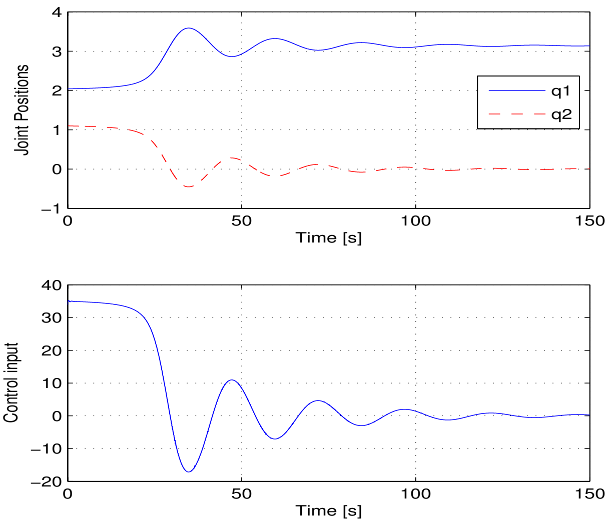

Fig. 2. The pendubot in completely upright position.

In the second simulation, the desired position was $q_{d_1} = \pi - 1.1 = 2.04$ [rad], and we have chosen an initial configuration $[q_1(0) \;\; q_2(0) \;\; p_1(0) \;\; p_2(0)]^T = [\pi \;\; 0 \;\; 0 \;\; 0]^T$. Notice that we have inverted the conditions of the first simulation. Now, we are interested in to carry to the pendubot around the upright position, starting from a completely upright position. The pictures in Fig. 3 show the temporal evolution of joint positions and the control input, and we can see as the joint positions q_1 and q_2 converge toward the desired equilibrium $[q_1 \;\; q_2 \;\; p_1 \;\; p_2]^T = [(\pi - 1.1) \;\; 1.1 \;\; 0 \;\; 0]^T$.

5. CONCLUSIONS

We have presented the IDA–PBC for a class of pendubot systems. The procedure of design follows a novel strategy shown in Acosta *et al.* [2005], that convert a set of PDE's into algebraic equations, through a suitable assignment of the desired structure in the J_2 matrix and the incorporation of the $\mathcal{A}$ matrix. Simulation results illustrate the performance of the proposed control system.

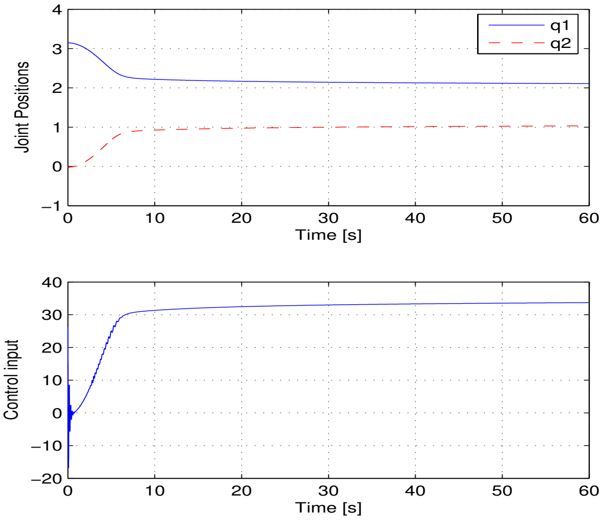

Fig. 3. The pendubot around the upright configuration.

REFERENCES

J. A. Acosta, R. Ortega, A. Astolfi and A. Mahindrakar. Interconnection and damping assignment passivity-based control of mechanical systems with underactuation degree one. *IEEE Transactions on Automatic Control*, **Vol. 50**, **No. 12**, December 2005.

R. Ortega, M. W. Spong, F. Gómez-Estern and G. Blankenstein, Stabilization of a class of underactuated mechanical systems via interconnection and damping assignment. *IEEE Transactions on Automatic Control*, **Vol. 47**, **No. 8**, pp. 1213–1233, August 2002.

M. W. Spong and D. Block. *The Pendubot: A mechatronic system for control research and education.* 34th IEEE Conf. Decision and Control, pp. 555–557, New Orleans, LA, December 1995

M. Wang-Sheng and L. Juang-Shan. *Backstepping control design of underactuated systems: A pendubot case study.* Proceedings of 2006 Automatic Control Conference, St. John's University, Tamsui, Taiwan, November 10–11, 2006.